

Minimal Control of Constrained, Partially Controllable & Observable Linear Systems*

Edwin Mora * Florian Steinke *

* *Energy Information Networks and Systems, Technische Universität Darmstadt, {edwin.mora, florian.steinke}@eins.tu-darmstadt.de*

Abstract: We aim at developing control strategies for constrained linear systems without requiring full system controllability and observability. Given a fixed, potentially small set of actuators and sensors, we first design a static affine-linear output feedback controller that guarantees both the asymptotic stability of the closed-loop system and the adherence of the steady state to a set of linear inequality constraints in the presence of interval-bounded, constant inputs. Subsequently, the derived method is used to find the minimum number of actuators and sensors with which one can fulfill such partial controllability and observability requirements. The approach is applied to electrical power networks modeled as a set of linearly coupled oscillators.

Keywords: Controllability, linear output feedback, optimization, resilience

1. INTRODUCTION

Controllable systems can be steered from any initial state to any desired state in finite time. Observable systems similarly allow the reconstruction of the exact initial state from finite time observations. While generally desirable, these conditions may often not be achievable for large, distributed systems, especially in situations with limited communication resources. Such conditions might, for example, arise in smart power systems through natural disasters or cyber-attacks. To increase the operational resilience of the network, we therefore aim at a weaker notion of controllability and observability that is still useful but allows for a strongly reduced number of actuator and measurement devices. Apart from resilience benefits, this also reduces the cost and effort for controlling the system in normal operation.

In this work, we investigate minimal realizations of static affine-linear output feedback controllers that guarantee asymptotic stability for linear systems, i.e., that a steady state of the system is approached for constant external conditions. Instead of steering the final state to a single target point, we define a larger target region and guarantee that the steady state is within this region, without being able to exactly identify the final state given the available measurement information. The target region is defined through a set of linear inequality constraints. The inputs to the system, both the controlled ones as well as the disturbance inputs, are assumed to be bounded. Contrary to available control techniques based on invariant sets (Dorea, 2009), we do not restrict the state trajectories to be within the target region at all times. This may allow to design a control law requiring much fewer resources.

Nevertheless, our design target is reasonable in many practical situations. E.g., in power systems, generator, transformer, or line capacity constraints limit system states and inputs, and short-term violations can often be accepted if the steady states are admissible (Carne et al., 2015; Sanz et al., 2017).

We thus address two tasks in this paper: 1) how to design a static affine-linear output feedback controller that fulfills the two above described conditions, and 2) how to select the minimum number of actuators and sensors required to achieve such a resilient design.

The first task is challenging due the simultaneous consideration of asymptotic stability, steady state performance, and bounded states and/or inputs. While traditional output feedback \mathcal{H}_∞ synthesis methods already provide an agreement between stability and performance (Petersen and Tempo, 2014), they cannot straightforwardly integrate state or input limits. This also applies to control energy minimizing approaches (Li et al., 2018; Lindmark and Altafini, 2018). When constraints are given, (stochastic) model predictive control and multi-shooting methods based on interior point optimization are often used to compute control policies that minimize a determined cost (Calafiore and Fagiano, 2013; Farina et al., 2016). However, such methods require complete state information and are computationally demanding.

The second research question is an instance of the well-known *optimal input/output selection problem*, an active research subject in the context of controlling complex networks (Liu and Barabási, 2016). Pequito et al. (2016) describe an efficient algorithm to determine the structural controllability of complex networks. Chang et al. (2018) address minimal actuator selection to design a static state feedback controller that ensures \mathcal{L}_∞ -stability. In addition, simultaneous minimal input/output selection via static output feedback has been addressed by Nugroho et al. (2018). Li et al. (2018) study the target controllability

* This work was sponsored by the German Federal Ministry of Education and Research in project AlgoRes, grant no. 01jS18066A. It has been performed in the context of the LOEWE center emergenCITY. © 2020 the authors. This work has been accepted to IFAC for publication under a Creative Commons Licence CC-BY-NC-ND.

of networked dynamical systems modeled as undirected graphs, in which only a subset of network states are steered towards a desired objective. However, all above proposed methods do not consider steady state restrictions on inputs or states. In a related work (Mora and Steinke, 2020), we study input/output selection for constrained static linear systems. The present paper extends these ideas to linear time-invariant systems and also addresses the stability of the resulting closed-loop system.

This paper is organized as follows. In Sec. 2, we provide a formal problem statement. We present an efficient method for the design of the desired controller based on linear and semidefinite programming in Sec. 3, first for fixed sets of controlled inputs and measurements. The approach is then used to develop an iterative algorithm that minimizes the number of required actuators and sensors in Sec. 4. In Sec. 5, we demonstrate the resulting algorithms for two illustrative power systems, before concluding in Sec. 6.

2. PROBLEM STATEMENT

We consider the linear time invariant system

$$\begin{aligned}\dot{\mathbf{x}}(t) &= \mathbf{A}\mathbf{x}(t) + \mathbf{B}\mathbf{u}(t), \\ \mathbf{y}(t) &= \mathbf{C}\mathbf{x}(t)\end{aligned}\quad (1)$$

with time $t \in \mathbb{R}_{\geq 0}$, state $\mathbf{x}(t) \in \mathbb{R}^N$, potential control inputs $\mathbf{u}(t) \in \mathbb{R}^L$, potential measurements $\mathbf{y}(t) \in \mathbb{R}^P$, and matrices of appropriate dimensions. It is presupposed that \mathbf{A} is non-singular and that the system is fully controllable and fully observable, if all inputs and outputs are used.

Now, let the set of possible control inputs $\mathbf{u}(t)$ be partitioned into the *controlled* inputs $\mathbf{u}_c(t)$, for which we will design a controller in the following, and the *free* inputs $\mathbf{u}_f(t)$, that are left free to be determined either by other users, cooperative or malicious, by fixed external conditions, or at random. The index set of the controlled variables is denoted by \mathcal{C} . Similarly, we partition the set of possible measurements $\mathbf{y}(t)$ into the *monitored* measurements $\mathbf{y}^m(t)$, that are used as inputs to the control law, and the *unmonitored* variables $\mathbf{y}^u(t)$, that are not required for the controller and may or may not be recorded in practice. The index set of the monitored variables is denoted by \mathcal{M} .

The defined partitions of $\mathbf{u}(t)$ and $\mathbf{y}(t)$ allow to partition \mathbf{B} and \mathbf{C} along their columns or rows as well, yielding

$$\begin{aligned}\mathbf{B}\mathbf{u}(t) &= \mathbf{B}_c\mathbf{u}_c(t) + \mathbf{B}_f\mathbf{u}_f(t), \\ \begin{bmatrix} \mathbf{y}^m(t) \\ \mathbf{y}^u(t) \end{bmatrix} &= \begin{bmatrix} \mathbf{C}^m \\ \mathbf{C}^u \end{bmatrix} \mathbf{x}(t).\end{aligned}$$

Note that we do not require the pair $(\mathbf{A}, \mathbf{B}_c)$ to be (fully) controllable or the pair $(\mathbf{A}, \mathbf{C}^m)$ to be (fully) observable, i.e., Kalman rank conditions for controllability and/or observability may not be fulfilled. Given the above definitions, we choose the desired control law as an affine-linear static output feedback

$$\mathbf{u}_c(t; \mathbf{S}, \mathbf{w}) = \mathbf{S}\mathbf{y}^m(t) + \mathbf{w}, \quad (2)$$

with gain $\mathbf{S} \in \mathbb{R}^{|\mathcal{C}| \times |\mathcal{M}|}$ and offset $\mathbf{w} \in \mathbb{R}^{|\mathcal{C}|}$. Hereby, $|\mathcal{C}|$ and $|\mathcal{M}|$ denote the cardinality of \mathcal{C} and \mathcal{M} , respectively. The control law shall guarantee the asymptotic stability of the resulting closed-loop system, characterized by the matrix $\tilde{\mathbf{A}}(\mathbf{S}) = \mathbf{A} + \mathbf{B}_c\mathbf{S}\mathbf{C}^m$. This implies that the system will

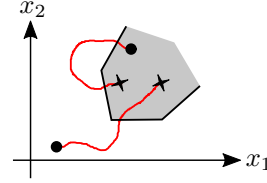


Fig. 1. From any (typically unknown) starting point (circles), the closed-loop system shall converge for fixed external conditions to a steady state (crosses) that may not be fully observable but is guaranteed to be within a given convex polyhedron (shaded).

settle to a steady state for constant free inputs. According to Lyapunov stability theory (Lyapunov, 1992), the system $\dot{\mathbf{x}}(t) = \tilde{\mathbf{A}}(\mathbf{S})\mathbf{x}(t)$, is asymptotically stable if there exists a positive definite matrix $\mathbf{P} \in \mathbb{R}^{N \times N}$ for which

$$\mathbf{P}\tilde{\mathbf{A}}(\mathbf{S}) + \tilde{\mathbf{A}}^T(\mathbf{S})\mathbf{P} \prec \mathbf{0}. \quad (3)$$

Given range-limited constant values for the free inputs $\mathbf{u}_f(t)$, it is additionally desired that the resulting control system fulfills a set of linear inequality constraints in steady state. Let \mathbf{x} , \mathbf{u} , and \mathbf{y} represent the steady state values of $\mathbf{x}(t)$, $\mathbf{u}(t)$, and $\mathbf{y}(t)$, respectively. Moreover, let $\mathbf{u} \in \mathcal{U}$, where \mathcal{U} is a priori known and can be partitioned as $\mathcal{U} = \mathcal{U}_c \times \mathcal{U}_f$. We study the case where \mathcal{U} is expressed as a product of intervals, i.e., $\mathcal{U} = [\underline{u}_1, \bar{u}_1] \times \dots \times [\underline{u}_L, \bar{u}_L]$.

The control target is then to maintain the steady state vector \mathbf{x} inside the convex polyhedron

$$\mathcal{X} = \{\mathbf{x} \in \mathbb{R}^N : \mathbf{E}\mathbf{x} \leq \mathbf{b}\}, \quad (4)$$

for all $\mathbf{u}_f \in \mathcal{U}_f$, where $\mathbf{E} \in \mathbb{R}^{K \times N}$ and $\mathbf{b} \in \mathbb{R}^K$, such as shown in Fig. 1. Since we assume that \mathbf{A} is non-singular, steady state conditions imply that

$$\mathbf{x} = -\mathbf{A}^{-1}(\mathbf{B}_c\mathbf{u}_c + \mathbf{B}_f\mathbf{u}_f) \quad (5)$$

and that we can express $\mathbf{E}\mathbf{x} \leq \mathbf{b}$ equivalently in terms of both \mathbf{u}_c and \mathbf{u}_f as

$$-\mathbf{E}\mathbf{A}^{-1}(\mathbf{B}_c\mathbf{u}_c + \mathbf{B}_f\mathbf{u}_f) \leq \mathbf{b}. \quad (6)$$

Now define $\mathbf{M}_c^m = -\mathbf{C}^m\mathbf{A}^{-1}\mathbf{B}_c$ and $\mathbf{M}_f^m = -\mathbf{C}^m\mathbf{A}^{-1}\mathbf{B}_f$. Equation (5) implies that $\mathbf{y}^m = \mathbf{M}_c^m\mathbf{u}_c + \mathbf{M}_f^m\mathbf{u}_f$ and that the steady state value of the controlled inputs \mathbf{u}_c can be expressed based only on the steady state value of the free inputs \mathbf{u}_f as

$$\mathbf{u}_c(\mathbf{u}_f; \mathbf{S}, \mathbf{w}) = \hat{\mathbf{S}}\mathbf{M}_f^m\mathbf{u}_f + \hat{\mathbf{w}}, \quad (7)$$

with

$$\hat{\mathbf{S}} = (\mathbf{I} - \mathbf{S}\mathbf{M}_c^m)^{-1}\mathbf{S}, \quad \hat{\mathbf{w}} = (\mathbf{I} - \mathbf{S}\mathbf{M}_c^m)^{-1}\mathbf{w}. \quad (8)$$

This representation of the control law has the advantage of simplifying the design process as we will discuss below. It also allows us to define the admissibility of the control law non-recursively as follows.

Definition 1. (Admissible control law). The control law (2) determined through \mathbf{S}, \mathbf{w} is steady state admissible if

$$\forall \mathbf{u}_f \in \mathcal{U}_f : \mathbf{u}_c(\mathbf{u}_f; \mathbf{S}, \mathbf{w}) \in \mathcal{U}_c \wedge \quad (9)$$

$$\mathbf{\Lambda}_c\mathbf{u}_c(\mathbf{u}_f; \mathbf{S}, \mathbf{w}) + \mathbf{\Lambda}_f\mathbf{u}_f \leq \mathbf{b}. \quad (10)$$

with $\mathbf{\Lambda}_c = -\mathbf{E}\mathbf{A}^{-1}\mathbf{B}_c$ and $-\mathbf{E}\mathbf{A}^{-1}\mathbf{B}_f$.

This allows us to formally state the optimization tasks we aim to solve in this work.

Problem 1. For fixed sets \mathcal{C} and \mathcal{M}

$$\begin{aligned} & \text{find } \mathbf{S}, \mathbf{w} \text{ of size corresponding to } \mathcal{C} \text{ and } \mathcal{M} \\ & \text{s.t. } \tilde{\mathbf{A}}(\mathbf{S}) \text{ is asymptotically stable and} \\ & \quad \mathbf{u}_c(\mathbf{u}_f; \mathbf{S}, \mathbf{w}) \text{ is steady state admissible.} \end{aligned} \quad (11)$$

Problem 2. Find the set of controllers \mathcal{C} and measurements \mathcal{M} that solves

$$\begin{aligned} & \min_{\mathcal{C}, \mathcal{M}} |\mathcal{C}| + \gamma |\mathcal{M}| \\ & \text{s.t. } \exists \mathbf{S}, \mathbf{w} \text{ of size corresponding to } \mathcal{C} \text{ and } \mathcal{M} \\ & \quad \text{that solve Problem 1.} \end{aligned} \quad (12)$$

The cost of placing a sensor is weighted by $0 \leq \gamma \leq 1$ since it will typically be smaller than implementing a full actuator. One could additionally incorporate into the objective the varying efforts and costs for controlling certain elements or acquiring certain measurements. Instead of just weighting the total number of controllers and measurements we would then determine an individual weight for each element separately. While we do not follow this idea below, all algorithms could readily be adapted.

Remark 1. For singular \mathbf{A} , the approach can be extended via the Moore–Penrose pseudo inverse \mathbf{A}^+ , if the kernel of \mathbf{A} is also in the kernel of \mathbf{C}^m and \mathbf{E} . The undetermined dimensions in (5) are then irrelevant for the critical conditions (9) and (10). This assumption is fulfilled, e.g., for the power systems example below.

3. CONTROLLER DESIGN FOR FIXED \mathcal{C} AND \mathcal{M}

3.1 Guaranteeing Steady State Admissibility

A steady state admissible controller parametrized by \mathbf{S} and \mathbf{w} has to fulfill the two conditions of Definition 1. These are formulated using the all-quantor concerning the free inputs \mathbf{u}_f . If used directly as side conditions in an optimization problem to determine the best controller, this would result in infinitely many constraints. In the following, we reformulate the constraints such that they yield a small set of linear conditions. According to Definition 1, the transformed control law (7) must fulfill

$$\underbrace{\begin{bmatrix} \mathbf{\Lambda}_c \hat{\mathbf{S}} \mathbf{M}_f^m + \mathbf{\Lambda}_f \\ \hat{\mathbf{S}} \mathbf{M}_f^m \\ -\hat{\mathbf{S}} \mathbf{M}_f^m \end{bmatrix}}_{\hat{\mathbf{A}}(\hat{\mathbf{S}})} \mathbf{u}_f + \underbrace{\begin{bmatrix} \mathbf{\Lambda}_c \\ \mathbf{I} \\ -\mathbf{I} \end{bmatrix}}_{\mathbf{F}} \hat{\mathbf{w}} - \underbrace{\begin{bmatrix} \mathbf{b} \\ \bar{\mathbf{u}}_c \\ -\mathbf{u}_c \end{bmatrix}}_{\mathbf{l}} \leq \eta \underbrace{\begin{bmatrix} \mathbf{1} \\ \cdot \\ \cdot \end{bmatrix}}_{\mathbf{v}}, \quad (13)$$

where we introduced $\eta \in \mathbb{R}$ as an indicator of how far the system is from violating the first steady state constraint, $\mathbf{1}$ is a vector of ones of suitable dimension, and \cdot a vector of zeros. In this context, a control law is steady state admissible if $\eta \leq 0$. Guaranteeing (13) for all $\mathbf{u}_f \in \mathcal{U}_f$ can be achieved by considering only the maximum of the left hand side expression. Let $\hat{K} = K + 2|\mathcal{C}|$ be the number of rows of $\hat{\mathbf{A}}(\hat{\mathbf{S}})$ and $N_f = N - |\mathcal{C}|$ the number of free inputs. We can introduce a tight upper bound on $\hat{\mathbf{A}}(\hat{\mathbf{S}})\mathbf{u}_f$ via a matrix $\mathbf{H} \in \mathbb{R}^{\hat{K} \times N_f}$, whose entries fulfill

$$\begin{aligned} H_{ij} & \geq \hat{\Lambda}_{ij}(\hat{\mathbf{S}}) \bar{u}_{fj}, \quad \forall i = 1, \dots, \hat{K}, \forall j = 1, \dots, N_f, \\ H_{ij} & \geq \hat{\Lambda}_{ij}(\hat{\mathbf{S}}) \underline{u}_{fj}, \quad \forall i = 1, \dots, \hat{K}, \forall j = 1, \dots, N_f. \end{aligned} \quad (14)$$

The upper bound of $\hat{\mathbf{A}}(\hat{\mathbf{S}})\mathbf{u}_f$ is then given by $\mathbf{H}\mathbf{1}$. Condition (13) is thus equivalent to

$$\mathbf{H}\mathbf{1} + \mathbf{F}\hat{\mathbf{w}} - \mathbf{l} \leq \eta \mathbf{v}. \quad (15)$$

This allows us computing the controller with the minimum possible value of η for given \mathcal{M} and \mathcal{C} via the following linear program (LP)

$$\begin{aligned} & \min_{\eta, \mathbf{H}, \hat{\mathbf{S}}, \hat{\mathbf{w}}} \eta \\ & \text{s.t. } \mathbf{H}\mathbf{1} + \mathbf{F}\hat{\mathbf{w}} - \mathbf{l} \leq \eta \mathbf{v}, \\ & H_{ij} \geq \hat{\Lambda}_{ij}(\hat{\mathbf{S}}) \bar{u}_{fj}, \quad \forall i = 1, \dots, \hat{K}, \forall j = 1, \dots, N_f, \\ & H_{ij} \geq \hat{\Lambda}_{ij}(\hat{\mathbf{S}}) \underline{u}_{fj}, \quad \forall i = 1, \dots, \hat{K}, \forall j = 1, \dots, N_f. \end{aligned} \quad (16)$$

We recover the original controller parameters by solving for \mathbf{S} and \mathbf{w}

$$\mathbf{S} = \hat{\mathbf{S}}(\mathbf{I} + \mathbf{M}_c^m \hat{\mathbf{S}})^{-1}, \quad \mathbf{w} = (\mathbf{I} - \mathbf{S} \mathbf{M}_c^m) \hat{\mathbf{w}}. \quad (17)$$

Remark 2. Note that, particularly in large scale applications, there may be several steady state constraints, i.e., rows of $\mathbf{\Lambda} = -\mathbf{E}\mathbf{A}^{-1}\mathbf{B}$ and corresponding entries of \mathbf{b} in condition (10), that are not violated by any realization of \mathbf{u} . Hence, when optimizing over \mathcal{C} and \mathcal{M} , we only take into account the rows of $\mathbf{\Lambda}$, for which a constraint violation is possible. To this end, we check for the i -row of $\mathbf{\Lambda}$ whether $\max(\mathbf{\Lambda}_i \cdot \mathbf{u} - b_i) > 0$ using the available bounds of \mathbf{u} .

3.2 Guaranteeing Asymptotic Stability

Determining the control law $\mathbf{u}_c(t; \mathbf{S}, \mathbf{w})$ via the LP (16) does not guarantee the stability of the resulting closed-loop system, which can be shown by counterexample. However, our experiments showed that asymptotically stable configurations are obtained in many cases. This can efficiently be checked by computing the maximum real part of the eigenvalues of the closed-loop dynamics $\tilde{\mathbf{A}}(\mathbf{S})$.

In cases where the resulting control system is not stable this can be enforced by solving

$$\begin{aligned} & \min_{\eta, \mathbf{H}, \hat{\mathbf{S}}, \hat{\mathbf{w}}, \mathbf{S}, \mathbf{w}, \mathbf{P}} \eta \\ & \text{s.t. conditions (14), (15), (17),} \\ & \quad \mathbf{P} \tilde{\mathbf{A}}(\mathbf{S}) + \tilde{\mathbf{A}}^T(\mathbf{S}) \mathbf{P} \prec \mathbf{0}, \\ & \quad \mathbf{P} \succ \mathbf{0}, \end{aligned} \quad (18)$$

i.e., we use Lyapunov inequality (3) as an additional constraint. Since equations (17) are non-linear if both $\hat{\mathbf{S}}, \hat{\mathbf{w}}$ and \mathbf{S}, \mathbf{w} are free optimization variables, this optimization problem is a bilinear matrix inequality (BMI). It is non-convex, but can be optimized locally. We adapt the *path-following* method proposed by Hassibi et al. (1999) and iteratively improve the stability of the closed-loop system. The method assumes that the actuators have limited authority, and hence shift the eigenvalues of the system only slightly in one step. This enables us to solve a linearized form of (18) in each iteration as a convex linear matrix inequality (LMI).

First, we take the solution of LP (16) as initial guess, obtaining the initial values $\hat{\mathbf{S}}_0, \hat{\mathbf{w}}_0$. Using equations (17), we then compute initial values for the control parameters \mathbf{S}_0 and \mathbf{w}_0 . Next, we analyze the effect of *small* perturbations around $\hat{\mathbf{S}}_0, \hat{\mathbf{w}}_0, \mathbf{S}_0$, and \mathbf{w}_0 on equations (17). We thus consider the substitutions

$$\begin{aligned} \hat{\mathbf{S}} & = \hat{\mathbf{S}}_0 + \delta \hat{\mathbf{S}}, & \mathbf{S} & = \mathbf{S}_0 + \delta \mathbf{S}, \\ \hat{\mathbf{w}} & = \hat{\mathbf{w}}_0 + \delta \hat{\mathbf{w}}, & \mathbf{w} & = \mathbf{w}_0 + \delta \mathbf{w}, \end{aligned} \quad (19)$$

where the δ -terms represent such small perturbations. By applying substitutions (19) on equations (17), we obtain linear relations with respect to the perturbation terms, i.e.,

$$\begin{aligned} (\mathbf{I} - \mathbf{S}_0 \mathbf{M}_c^m) \delta \hat{\mathbf{S}} &= \delta \mathbf{S} (\mathbf{I} + \mathbf{M}_c^m \hat{\mathbf{S}}_0), \\ \mathbf{S}_0 \mathbf{M}_c^m \delta \hat{\mathbf{w}} &= -\delta \mathbf{S} \mathbf{M}_c^m \hat{\mathbf{w}}_0. \end{aligned} \quad (20)$$

Although \mathbf{S}_0 yields initially an unstable closed-loop system $\tilde{\mathbf{A}}_0 = \tilde{\mathbf{A}}(\mathbf{S}_0)$, we can still find a Lyapunov matrix \mathbf{P}_0 that proofs its largest growth rate, which is determined by the maximum real part over all eigenvalues of $\tilde{\mathbf{A}}_0$, here denoted by ρ_0 . For small $\epsilon > 0$ we can find \mathbf{P}_0 by solving the LMI

$$\begin{aligned} \min_{\kappa, \mathbf{P}_0} \quad & \kappa \\ \text{s.t.} \quad & \mathbf{I} \prec \mathbf{P}_0 \prec \kappa \mathbf{I}, \\ & \tilde{\mathbf{A}}_0^T \mathbf{P}_0 + \mathbf{P}_0 \tilde{\mathbf{A}}_0 \preceq 2(\rho_0 + \epsilon) \mathbf{P}_0, \end{aligned}$$

where the optimization variable $\kappa \in \mathbb{R}_{\geq 0}$ ensures that the obtained \mathbf{P}_0 has the smallest condition number. We can now linearize Lyapunov inequality (3) by introducing the substitutions $\mathbf{P} = \mathbf{P}_0 + \delta \mathbf{P}$, $\rho = \rho_0 + \delta \rho$, and neglecting second order perturbation terms. We obtain

$$\begin{aligned} \tilde{\mathbf{A}}_0^T (\mathbf{P}_0 + \delta \mathbf{P}) + (\mathbf{P}_0 + \delta \mathbf{P}) \tilde{\mathbf{A}}_0^T + \mathbf{P}_0 \mathbf{B}_c \delta \mathbf{S} \mathbf{C}^m + \\ (\mathbf{B}_c \delta \mathbf{S} \mathbf{C}^m)^T \mathbf{P}_0 \preceq 2\rho (\mathbf{P}_0 + \delta \mathbf{P}) + 2\delta \rho \delta \mathbf{P}_0. \end{aligned} \quad (21)$$

where $\delta \rho$ is fixed and chosen to be *small*. This results in the following semidefinite program

$$\begin{aligned} \min_{\eta, \mathbf{H}, \delta \hat{\mathbf{S}}, \delta \hat{\mathbf{w}}, \delta \mathbf{S}, \delta \mathbf{P}} \quad & \eta \\ \text{s.t.} \quad & \text{conditions (14), (15), (20), (21),} \\ & \mathbf{P}_0 + \delta \mathbf{P} \succeq \mathbf{0}, \end{aligned} \quad (22)$$

In case we obtain a steady state admissible solution, i.e., $\eta \leq 0$, we update the control parameters according to the obtained perturbations. This process is repeated iteratively until an asymptotically stable closed-loop system is obtained. If LMI (22) is infeasible or $\eta > 0$, the process is stopped and different sets for \mathcal{C} and \mathcal{M} are considered.

4. DETERMINING MINIMAL INPUT/OUTPUT SETS

To solve problem 2, i.e., determining the minimal feasible sets \mathcal{C} and \mathcal{M} , we now use the above described controller design procedure as a subroutine in a greedy *hill climbing* approach. Thus, we proceed iteratively from initially empty sets \mathcal{C} and \mathcal{M} , adding one element at a time. Since we want to measure the optimization progress also for combinations \mathcal{C} and \mathcal{M} for which no controller can be found that satisfies the desired design properties, we extend the minimization objective to

$$J(\mathcal{C}, \mathcal{M}) = |\mathcal{C}| + \gamma |\mathcal{M}| + \mu \max(\eta, \rho, 0), \quad (23)$$

where η corresponds to the steady state admissibility indicator defined in (13), and ρ to the maximum real part of the eigenvalues of $\tilde{\mathbf{A}}$. $\mu > 0$ is a weighting factor that penalizes the infeasibility of \mathcal{C} and \mathcal{M} . We choose $\mu \gg 1$ to steer the iteration quickly towards feasible solutions.

In each iteration we compute the objective value (23) for all sets \mathcal{M}' or \mathcal{C}' that can be generated by adding one element to either \mathcal{M} or \mathcal{C} . We then choose the step which yields the largest improvement of the objective value (23). As soon as the sets of controllers and measurements are feasible, we stop the iteration.

For large scale applications, the design of a stabilizing controller for each instance of \mathcal{C} and \mathcal{M} via the approach described in Section 3.2 is computationally demanding. For this reason, we recommend to grow \mathcal{C} and \mathcal{M} first

by solving LP (16) until $\eta \leq 0$ is reached and only then optimize stability. Moreover, if there is a steady state admissible controller among the candidates that implies a stable close-loop system without additional action, we can take this one and avoid further efforts.

Remark 3. It is well known that the solution of this greedy approach depends on the selection of the starting point, which also affects the total computation time. Starting with empty sets aims at selecting the most important controllers and measurements during the first iterations. In previous work (Mora and Steinke, 2020), we show that for a case corresponding to $-\mathbf{C}\mathbf{A}^{-1}\mathbf{B} = \mathbf{I}$, which can be shown to be practical at least for some examples, the minimal sets \mathcal{C} and \mathcal{M} fulfilling a weaker feasibility condition can be computed by solving a single mixed-integer linear program. While the obtained sets may be slightly too small, they can be a good starting point for the hill climbing procedure, leading to faster execution.

5. APPLICATION TO LINEAR POWER SYSTEMS

In this section, we show the potential of the above developed algorithms to design wide-area controllers for electrical power systems. After a brief description of the dynamics of power systems in the linear regime, we present the designs for 1) an introductory microgrid and 2) a modified version of the standard IEEE 57 bus network.

5.1 Linear Power Grids

We analyze electrical networks with n electrical buses connected by l transmission lines under the common *DC power flow* assumptions (Kundur et al., 1994). The power grid with integrated primary control action can then be modeled around its nominal operating point as a network of coupled oscillators subject to the linear swing equation

$$\mathbf{J}\ddot{\boldsymbol{\theta}}(t) + \mathbf{K}\dot{\boldsymbol{\theta}}(t) + \mathbf{B}_l\boldsymbol{\theta}(t) = \mathbf{p}(t), \quad (24)$$

where $\boldsymbol{\theta}(t) \in \mathbb{R}^n$ symbolizes the vector of voltage angles, and $\mathbf{p}(t) \in \mathbb{R}^n$ the vector of set points for the active power injections. We assume that both the inertia $\mathbf{J} \in \mathbb{R}^{n \times n}$ and primary control $\mathbf{K} \in \mathbb{R}^{n \times n}$ matrices are diagonal. Moreover, it is presupposed that $\mathbf{J} \succ \mathbf{0}$ and $\mathbf{K} \succeq \mathbf{0}$. The coupling matrix $\mathbf{B}_l \in \mathbb{R}^{n \times n}$ is given element-wise as $B_{l,jk} = -b_{jk}$ if $j \neq k$, and $B_{l,jj} = \sum_k b_{jk}$, with b_{jk} being the susceptance of the line connecting buses j and k .

By defining $\mathbf{x}(t) = \left[\boldsymbol{\theta}^T(t) \quad \dot{\boldsymbol{\theta}}^T(t) \right]^T$ and $\mathbf{u}(t) = \mathbf{p}(t)$, the state space representation of (24) is given by

$$\dot{\mathbf{x}}(t) = \underbrace{\begin{bmatrix} \cdot & \mathbf{I} \\ -\mathbf{J}^{-1}\mathbf{B}_l & -\mathbf{J}^{-1}\mathbf{K} \end{bmatrix}}_{\mathbf{A}} \mathbf{x}(t) + \underbrace{\begin{bmatrix} \cdot \\ \mathbf{J}^{-1} \end{bmatrix}}_{\mathbf{B}} \mathbf{u}(t), \quad (25)$$

where we use \cdot to denote a matrix of zeros with suitable dimensions. Quantities like the active power injected by generators or consumed by loads, the nodal frequencies, and the line power flows are potential measurements, that can all be extracted linearly from $\mathbf{x}(t)$. The nodal injections will be limited above and below by the technical capabilities of the connected generator or load. Similarly, line power flows and the grid frequency are typically subject to upper and lower bounds. This reasoning lets us define the structure of the linear inequalities $\mathbf{E}\mathbf{x} \leq \mathbf{b}$.

5.2 Introductory Microgrid

The considered microgrid consists of 3 generators supplying a demand of 5 MW. Fig. 2a shows the topology of the grid together with the capacity limits of each transmission line and each generator/load. The generator located at bus 4 provides primary reserve, with a droop of 4 MW/Hz. Nodal frequency deviations must not exceed ± 0.1 Hz.

We first assume that all transmission lines have a power transfer capacity of ± 10 MW, which is adequate to avoid grid limitations. It is presupposed that both the nodal power injections and the line flows are in the set of potential measurements. Nodal frequencies are not monitored. In this scenario, it is sufficient to control the generator located at bus 4 based on the power flowing between buses 2 and 3, in order to fulfill the steady state requirements. Note that the system is not fully controllable and observable, since both the observability and the controllability matrix have insufficient rank. We also simulate the dynamics of the network assuming that the free control inputs are manipulated at fixed time intervals, uniformly at random, and low-pass filtered. Fig. 2b shows how the resulting controller maintains the frequency deviations within the desired region in steady state, while occasional violations during the transition period can be observed.

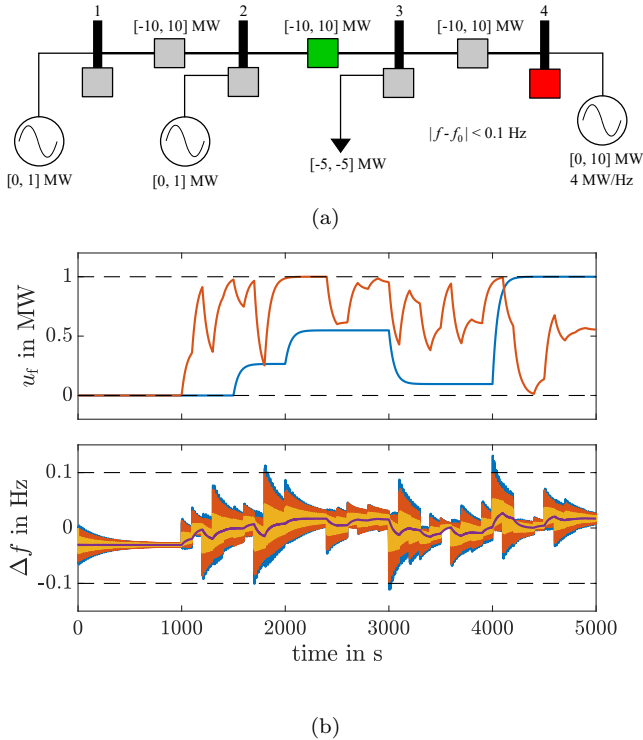


Fig. 2. Simple microgrid without active constraints on the transmission lines. (a) The gray boxes represent potential locations for the elements of \mathcal{C} and \mathcal{M} . The selected controllers and sensors correspond to the red and green boxes, respectively. (b) Top: External input $\mathbf{u}_f(t)$, i.e., trajectories of the uncontrolled generators 1 (blue) and 2 (red). Bottom: Resulting transient frequency deviations for all 4 buses.

Next, we constrain the power flowing between buses 2 and 3 to be within the interval $[-1, 1]$ MW. The resulting

minimum sets \mathcal{C} and \mathcal{M} are shown in Fig. 3. We see that in this case, the injection at bus 2 must additionally be controlled. Fig. 3 also presents an alternative steady state solution. When controlling the injection at bus 1 instead of the injection at bus 2, the solution of LP (16) is initially steady state admissible, but unstable in closed-loop. The system can, however, be stabilized with only one iteration of the path-following algorithm. Note that during the hill climbing we rarely required the stability improvement procedure. When screening the possible updates of \mathcal{C} and \mathcal{M} with the fast LP approach yielded steady state admissible candidates, at least one of them was typically already closed-loop stable.

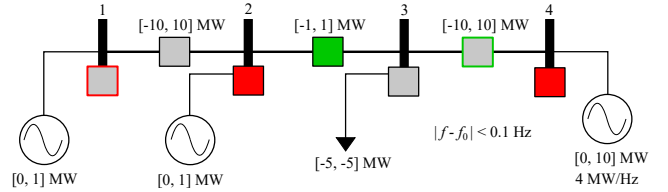


Fig. 3. Effect of adding an active constraint to the power flowing between buses 2 and 3. The colored frames denote alternative equivalent optimal solutions.

5.3 IEEE 57 bus test case

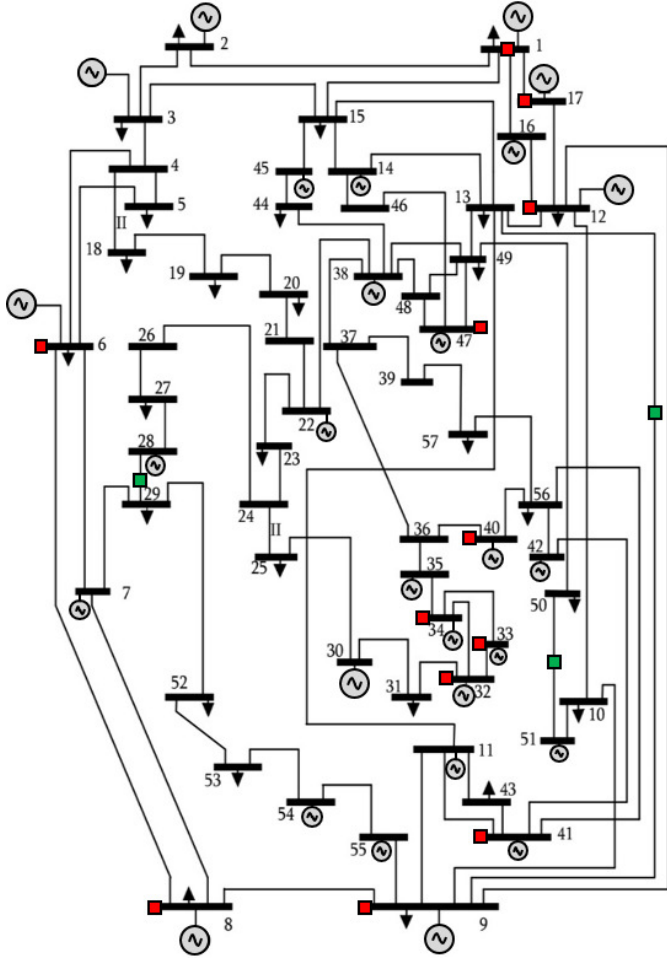
We now design the controller for the modified IEEE 57 bus power system, shown in Fig. 4a. It has 28 generators, 29 loads, and 80 transmission lines. The topology of the power system, the nominal load values, and generator capacities for producers located at buses $\{1, 2, 3, 6, 8, 9, 12\}$ were taken from Al-Roomi (2015). The capacity of the remaining generators are drawn from a uniform distribution within the interval $[0, 150]$ MW, and the capacity of the transmission lines is set to ± 100 MW. It is also presupposed that the power injections as well as the line flows are available as potential measurements. In addition, we admit 5% of uncertainty for each load in both directions. The maximum allowed frequency deviation is ± 0.2 Hz.

The obtained optimal sets for controlling this network are shown in Fig. 4a. We obtain that 12 generators must be controlled based on 3 line flow measurements in order to fulfill the two design specifications. Next, we simulate the time behavior of the system, manipulating the set-points of the non-controlled generators and loads as before, at fixed time intervals according to a uniform distribution and applying low-pass filtering. Fig. 4b shows that the local frequency deviations and the line flows remain within the desired region throughout the simulation time.

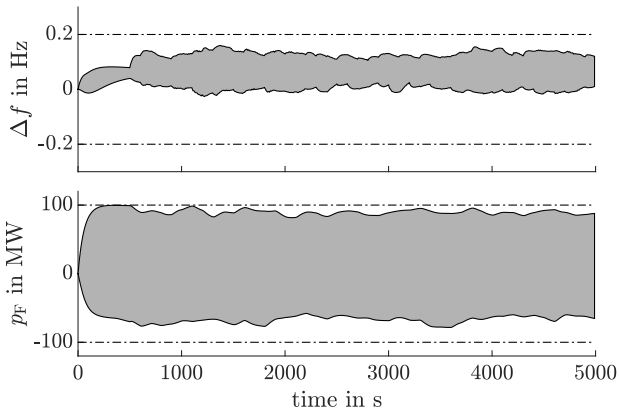
6. CONCLUDING REMARKS

The theoretic framework and the algorithms developed in this work allow to design a static output feedback controller that forces the steady state to fulfill a set of linear inequalities for interval-bounded, constant inputs and disturbances while keeping the resulting closed-loop system stable. While the stabilization of the system is typically achieved after few iterations of the path-following method, a convex stability condition in terms of the transformed control parameters $\hat{\mathbf{S}}$ and $\hat{\mathbf{w}}$ should be investigated in the future.

REFERENCES



(a)



(b)

Fig. 4. (a) Minimum sets \mathcal{C} and \mathcal{M} for the modified IEEE 57 bus power system. The location of the selected controllers and sensors is marked in red and green, respectively. (b) Time behavior of the transient frequency deviations (top) and the line flows (down) when the remaining non-controlled generators and loads are manipulated randomly within their operating limits. The area in gray encloses the time trajectories of all nodal frequencies and all line flows, the dashed lines mark their allowed range.

- Al-Roomi, A.R. (2015). Power flow test systems repository. URL <https://al-roomi.org/power-flow>.
- Calafiore, G.C. and Fagiano, L. (2013). Robust model predictive control via scenario optimization. *IEEE Transactions on Automatic Control*, 58(1), 219–224.
- Carne, G.D., Buticchi, G., Liserre, M., Marinakis, P., and Vournas, C. (2015). Coordinated frequency and voltage overload control of smart transformers. In *2015 IEEE Eindhoven PowerTech*. IEEE.
- Chang, C.Y., Martínez, S., and Cortés, J. (2018). Co-optimization of control and actuator selection for cyber-physical systems. *IFAC-PapersOnLine*, 51(23), 118–123.
- Dorea, C.E.T. (2009). Output-feedback controlled-invariant polyhedra for constrained linear systems. In *Proceedings of the 48th IEEE Conference on Decision and Control (CDC) held jointly with 2009 28th Chinese Control Conference*. IEEE.
- Farina, M., Giullioni, L., and Scattolini, R. (2016). Stochastic linear model predictive control with chance constraints—a review. *Journal of Process Control*, 44, 53–67.
- Hassibi, A., How, J., and Boyd, S. (1999). A path-following method for solving BMI problems in control. In *Proceedings of the 1999 American Control Conference*. IEEE.
- Kundur, P., Balu, N., and Lauby, M. (1994). *Power system stability and control*. EPRI power system engineering series. McGraw-Hill Education.
- Li, G., Deng, L., Xiao, G., Tang, P., Wen, C., Hu, W., Pei, J., Shi, L., and Stanley, H.E. (2018). Enabling controlling complex networks with local topological information. *Nature*, 8(4593).
- Li, J., Chen, X., Pequito, S., Pappas, G.J., and Preciado, V.M. (2018). Structural target controllability of undirected networks. In *2018 IEEE Conference on Decision and Control (CDC)*. IEEE.
- Lindmark, G. and Altafini, C. (2018). Minimum energy control for complex networks. *Nature*, 8(1).
- Liu, Y.Y. and Barabási, A.L. (2016). Control principles of complex systems. *Reviews of Modern Physics*, 88(3).
- Lyapunov, A.M. (1992). The general problem of the stability of motion. *International Journal of Control*, 55(3), 531–534.
- Mora, E. and Steinke, F. (2020). On the minimal set of controllers and sensors for linear power flow. *21st Power Systems Computation Conference (Accepted)*.
- Nugroho, S., Taha, A.F., Summers, T., and Gatsis, N. (2018). Simultaneous sensor and actuator selection/placement through output feedback control. In *2018 Annual American Control Conference*. IEEE.
- Pequito, S., Kar, S., and Aguiar, A.P. (2016). A framework for structural input/output and control configuration selection in large-scale systems. *IEEE Transactions on Automatic Control*, 61(2).
- Petersen, I.R. and Tempo, R. (2014). Robust control of uncertain systems: Classical results and recent developments. *Automatica*, 50(5), 1315–1335.
- Sanz, I.M., Judge, P.D., Spallarossa, C.E., Chaudhuri, B., and Green, T.C. (2017). Dynamic overload capability of VSC HVDC interconnections for frequency support. *IEEE Transactions on Energy Conversion*, 32(4).